Accepted Manuscript

Performance and stability improvements for dye-sensitized solar cells in the presence of luminescent coatings

Federico Bella, Gianmarco Griffini, Matteo Gerosa, Stefano Turri, Roberta Bongiovanni

PII: S0378-7753(15)00350-X

DOI: 10.1016/j.jpowsour.2015.02.105

Reference: POWER 20733

To appear in: *Journal of Power Sources*

Received Date: 17 November 2014

Revised Date: 23 January 2015

Accepted Date: 18 February 2015

Please cite this article as: F. Bella, G. Griffini, M. Gerosa, S. Turri, R. Bongiovanni, Performance and stability improvements for dye-sensitized solar cells in the presence of luminescent coatings, *Journal of Power Sources* (2015), doi: 10.1016/j.jpowsour.2015.02.105.

Performance and stability improvements for dye-sensitized solar cells in the presence of luminescent coatings

Federico **Bella**,[*,1] Gianmarco **Griffini**,[2] Matteo **Gerosa**,[1] Stefano **Turri**,[2] and Roberta **Bongiovanni**[1]

1) Department of Applied Science and Technology - DISAT, Politecnico di Torino, Corso Duca degli Abruzzi 24, 10129 Torino, Italy

2) Department of Chemistry, Materials and Chemical Engineering "Giulio Natta", Politecnico di Milano, Piazza Leonardo da Vinci 32, 20133 Milano, Italy

[*] Corresponding author: Federico Bella (E-mail federico.bella@polito.it; Tel: +39 0110904638; Contact details: affiliation 1)

ABSTRACT. Here we present how the sunlight radiation incident on a dye-sensitized solar cell (DSSC) can be shifted of a few tens of nanometers by means of an economical, easy to prepare and multifunctional photocurable fluoropolymeric light-shifting (LS) coating, to achieve both improved efficiency and device stability. By the introduction of a very small amount of a luminescent agent in the LS coating, the down-shifting of near-UV photons to higher wavelengths easily harvestable by the organic dye of a DSSC is successfully demonstrated. This optical effect not only results in an over 60% improvement of the power conversion efficiency of DSSC devices, but the UV light filtering action promoted by the luminescent agent also provides protection to the photosensitive DSSC components. This aspect, combined with a potential thermal shielding effect and the easy-cleaning behavior imparted to the coating by its fluorinated nature, leads to excellent device stability as evidenced from an aging test performed outdoors under real operating conditions for more than 2000 hours. Our study demonstrates that the use of light-cured multifunctional coatings with light management characteristics at the nanometer scale represents a new promising strategy to simultaneously increase the performance and durability of DSSC devices.

KEYWORDS. Dye-sensitized solar cell, Luminescent down shifting, Coating, Fluoropolymer, UV protection, Easy-cleaning.

1. INTRODUCTION

Dye-sensitized solar cells (DSSCs) have proven to be one of the most valuable third generation photovoltaic (PV) technology for the conversion of solar energy into electricity during the last twenty years [1]. The seminal work of O'Regan and Grätzel is the most cited article in the whole energy field [2], and more than 13,000 papers have been written to propose new materials, characterization techniques and large-scale implementation of DSSCs [3]. At present, efficiencies higher than 13% have been obtained on a laboratory scale [4], but also the manufacture of flexible devices [5], the design of unconventional electrodes [6], and the fabrication of hybrid cells [7] are research topics of great interest.

However, a few important aspects still need to be addressed in order to make DSSCs even more attractive and reliable on the global energy market. First of all, investigations have been carried out mostly on organometallic dyes, but metal-free organic dyes are getting increasing attention in view of obtaining market-competitive devices [8]. Organic dyes do not contain any rare or noble metal, thus generating fewer concerns about resource limits, and have recently demonstrated to be able to produce a 12.5% efficiency [9]. The second topic concerns the outdoor use of DSSCs, and therefore their resistance to meteorological phenomena, pollution and undesired UV radiation. Quite surprisingly, coatings have been developed almost exclusively for antireflective purposes, especially for silicon- and CdTe-based solar cells [10,11]. During the last two years, multifunctional coatings have also been designed for combined antireflective and self-cleaning purposes, and have been applied onto silicon and polymeric solar cells [12,13]. Even if polymers have been chosen as basic matter for coating preparation, also inorganic matrices (pure or mixed metal oxides) have been investigated [14]. However, despite the great academic and industrial efforts spent on DSSCs components, the development of functional coatings for improving the outdoor stability and performance of this type of third generation devices has been surprisingly neglected. Most of the research groups overlook this aspect, and only a small fraction of them apply a commercial antireflective coating on the fabricated PV cells [15]. Very recently, a couple of interesting works

has been proposed on this matter. Park *et al.* prepared a superhydrophilic nanoparticle-based coating to be applied as anti-fogging layer [16], while Heo *et al.* fabricated a hydrophobic nanopatterned coating with antireflective and self-cleaning properties [17]. We think that the impact of these seminal works may trigger the interest of the scientific community on a very far ignored aspect of DSSC technology. In particular, the great potential of fluorinated polymer matrices has yet to be exploited in the DSSC field. Indeed, fluorinated polymers are a class of high-performance materials that rely on the superior strength (higher dissociation energy) of the carbon-fluorine bond compared to the carbon-hydrogen bond to achieve excellent durability, weatherability, chemical and photochemical resistance [18,19,20]. The use of fluorinated polymer coatings for outdoor applications represents a consolidated way to achieve high weathering resistance and long-term durability in a variety of technological fields (e.g., architectural, nautical), and only very recently their application to the field of energy storage and conversion has also been demonstrated [21,22,23].

Our recent experimental research activities have been separately focused on the preparation of light-managing coatings for PV applications [23,24] and on the development of new materials for different PV technologies [25,26,27]. A very ambitious goal would be that of combining the ability of a coating to be easily-cleanable with a light-shifting (LS) effect promoted by the addition of an appropriate luminophore to the coating system. Considering this latter point, a few recent articles reported on the use of rare earths as UV or visible light shifters [28,29,30,31,32]. However, such systems have two major flaws: 1) The luminophores (Y_2WO_6:Ln^{3+}, $NaYF_4$:Yb^{3+}/Er^{3+}, CaZnOS:Eu^{2+}, Y_2O_3:Er^{3+}) are composed of rare and expensive inorganic elements; 2) Aging studies on devices including these LS systems are not presented, presumably because these inorganic materials are water soluble or suspendable, thus real outdoor applications are not conceivable. A first example of a stable luminescent system for DSSCs has been very recently proposed by our group, and consisted of a polymer coating containing an Europium complex as downshifter [33].

However, the presence of rare and expensive element such as Europium does not make this technology suitable for a large-scale trade.

In this work, we propose a multifunctional coating which can simultaneously be easy-cleaning and LS for application in organic DSSCs. In detail, the easy-cleaning ability is ascribed to the use of a fluoropolymeric matrix system that can be photocured in a few seconds, thus potentially enabling its use in large-scale production volumes. By the addition of a rare elements-free organic fluorophore, this coating is also able to serve as LS system by absorbing light in the UV portion of the solar spectrum and re-emitting it in the spectral region where the DSSC sensitizer shows a maximum absorption (Fig. 1). Since organic DSSC dyes often present a relatively narrow spectral breadth [34,35], our proof of concept shows the possibility to partly overcome this problem, by shifting otherwise-wasted and potentially harmful UV-photons to wavelengths suitable for absorption by the DSSC device. The optimization of the LS-DSSC system allowed us to improve by 62% the efficiency of a DSSC prepared with the organic dye D131. Moreover, thanks to the UV-screening action of the rare elements-free fluorophore used in the LS-coating presented in this work, the often detected photo-oxidative degradation of the organic dye [36] could be prevented. Accordingly, an aging test conducted for more than 2000 h in real outdoor conditions revealed the excellent stability of the new LS-DSSC system presented in this work compared to control devices.

Fig. 1 HERE

2. EXPERIMENTAL

2.1 Materials. The chloro-tri-fluoro-ethylene vinyl-ether (CTFE-VE) polymeric binder (Lumiflon LF-910LM) was obtained from Asahi Glass Company Ltd., while 2-isocyanatoethyl methacrylate (IEM) was obtained from Showa Denko K.K.. Both were used as received. The luminescent species employed in this work was Lumogen F Violet 570, purchased from BTC Europe.

As regards DSSC components, conducting glass plates (FTO glass, Fluorine doped Tin Oxide over-layer, sheet resistance 7 Ω sq^{-1}, purchased from Solaronix) were cut into 2 cm × 2 cm sheets and used as substrates for both the deposition of a TiO_2 porous film from a paste (DSL 18NR-AO, Dyesol) and the fabrication of platinized counter-electrodes. Sensitizing dye 2-[{4-[4-(2,2-diphenylethenyl)phenyl]-1,2,3,3a,4,8b-hexahydrocyclopento[b]indole-7-yl}methylidene]-cyanoacetic acid (D131) was purchased from Inabata Europe S.A.

All other reagents were purchased from Sigma Aldrich, unless otherwise stated.

2.2 Synthetic method. The CTFE-VE polymer was allowed to react with IEM to form the photocrosslinkable polyurethane precursor. In a typical synthesis, 40 g of CTFE-VE and 7.3 g of IEM were poured in stoichiometric ratio (OH/NCO = 1) into a three-necked round-bottomed flask equipped with a bubble condenser. Di-*n*-butyltin dilaurate (0.3 wt. %) was added successively to act as catalyst. The reaction was conducted in a nitrogen atmosphere and under vigorous magnetic stirring at 75 °C. The extent of reaction was controlled by monitoring the disappearance of the N=C=O stretching signal (2270 cm^{-1}) by means of FTIR spectroscopy, and was found to be completed after about 6 h. The final product was diluted with chloroform ($CHCl_3$) to the desired concentration.

2.3 UV-curing process. In order to perform the UV-curing process, photopolymer precursor was exposed to UV-light (35 mW cm^{-2}, as measured by means of a UV Power Puck® II radiometer, EIT) coming from a medium pressure mercury lamp equipped with an optical guide (LC8, Hamamatsu) for 60 s. The UV irradiation was carried out under nitrogen flux, to prevent quenching of free-radicals by atmospheric oxygen. Darocur 1173 (Ciba Specialty Chemicals) was used as the photoinitiator (3 wt. %). UV-exposed polymer films were immersed in $CHCl_3$ for 5 min to preliminary evaluate the extent of UV-curing. The conversion of the UV-curing reaction was monitored by FTIR by depositing a film of polymer precursor onto a KBr disk via spin-coating and subsequently irradiating it with UV light for a given amount of time, followed by quenching in an

ice bath to stop the curing reaction. The FTIR spectrum of the film was then collected. This procedure was repeated on the same polymer film for increasing UV-light exposure times, for a maximum of 120 s.

2.4 DSSC fabrication. Photoanodes preparation started with a cleaning process: FTO covered glasses were rinsed in acetone and ethanol in an ultrasonic bath for 10 min. Then, a TiO_2 paste layer with a circular shape was deposited on FTO by screen printing technique (AT-25PA, Atma Champ Ent. Corp.) and dried at 100 °C for 10 min on a hot plate. A sintering process at 525 °C for 30 min led to a nanoporous TiO_2 film with an average thickness of 8.5 µm, measured by profilometry (P.10 KLA-Tencor Profiler). The photoelectrodes were then soaked into a 0.5 mM D131 dye solution in a *tert*-butanol:acetonitrile 1:1 mixture for 5 h at ambient temperature, and finally washed with acetone to remove the unadsorbed dye. 0.5 mM of chenodeoxycholic acid (CDCA) as coadsorbent in the dye solution was added.

As regards the preparation of counter electrodes, 6 nm Pt thin films were deposited by sputtering (Q150T ES, Quorum Technologies Ltd) onto FTO glasses, previously cleaned with the same rinsing method described above.

For DSSC device fabrication, photoanode and counter electrode were assembled into a sealed sandwich type cell with a gap of a hot-melt ionomer film, Surlyn (60 µm, Du-Pont). The cell internal space was filled with electrolyte *via* vacuum backfilling. The liquid electrolyte consisted of 1-methyl-3-propylimidazolium iodide (MPII, 0.60 M), iodine (I_2, 50 mM), lithium iodide (LiI 0.10 M) and 4-*tert*-butylpyridine (TBP, 50 mM) in 3-methoxypropionitrile (MPN). The injection hole on the counter electrode was then sealed with a Surlyn sheet and a thin glass slice by heating.

The UV-curable photopolymer precursor was diluted to a concentration of 30 wt. % in $CHCl_3$. The amount of the luminescent species in the UV-curable fluoropolymer was varied between 0 wt. % and 10 wt. %. Each sealed DSSC was fixed onto a SPIN150 spin processor (SPS-Europe), and a few drops of the UV-curable precursor were placed on the external side of the photoanode. Samples

were spin-coated at 1000 rpm for 45 s with an acceleration equal to 25 rpm s^{-1}, and subsequently UV-cured as reported above. The final thickness of the coating was 35 μm, which preliminary tests proved to be the best value for our purposes.

2.5 Characterization techniques. UV-vis and fluorescence spectroscopy were performed on UV-cured LM-coatings deposited onto glass/quartz substrates by spin-coating (WS-400B-NPP Spin-Processor, Laurell Technologies Corp.) at 1000 rpm for 40 s in air. UV–vis absorption spectra were recorded in air at room temperature in transmission mode by means of an Evolution 600 UV–vis spectrophotometer (Thermo Scientific). Fluorescence emission spectra were recorded in air at room temperature on a Jasco FP-6600 spectrofluorometer. The excitation wavelength was λ_{exc} = 340 nm.

FTIR spectra were recorded in air at room temperature with a Nicolet 670-FTIR spectrophotometer.

TGA was performed on solid state samples using a Q500 TGA system (TA Instruments) from ambient temperature to 600 °C at a scan rate of 10 °C/min in air.

Static optical contact angle measurements on the LS coating were performed with an OCA 20 (DataPhysics) equipped with a CCD photo-camera and with a 500-μL Hamilton syringe to dispense liquid droplets. Measurements were taken at room temperature via the sessile drop technique. At least 20 measurements were performed in different regions on the surface of each coating and results were averaged. Water and diiodomethane were used as probe liquids.

PV measurements were performed on DSSC devices having active area of 0.78 cm^2 using a 0.16 cm^2 rigid black mask. I-V electrical characterizations under AM1.5G illumination (100 mW cm^{-2}, or 1 sun) were carried out using a class A solar simulator (91195A, Newport) and a Keithley 2440 source measure unit. All the measurements were carried out on at least three different fresh cells in order to verify the reproducibility of the obtained results, and the experimental results shown in the manuscript are the average of the three replicates. IPCE measurements were performed in DC mode using a 100-W QTH lamp (Newport) as light source and a 150-mm Czerny

Turner monochromator (Omni-λ 150, Lot-Oriel, Darmstadt, Germany). As regards devices aging, a standardized protocol for the evaluation of the stability of DSSCs is not present, thus a long-term weathering study was conducted under real outdoor conditions for about 3 months.

3. RESULTS AND DISCUSSION

In order to obtain the new functional coating system presented in this study, a new UV-curable polymeric precursor was developed, based on a chloro-trifluoro-ethylene vinyl-ether (CTFE-VE) fluoropolymer. In particular, the CTFE-VE polymer was reacted with 2-isocyanatoethyl methacrylate (IEM) to yield a fluoropolymeric precursor bearing photosensitive unsaturated moieties as pendant side groups attached to the main polymer chain. As schematically illustrated in Fig. 2A, this functionalization reaction leads to the formation of urethane bonds from the addition of the -N=C=O groups (IEM) to the -OH groups present in the fluoropolymer, the latter acting in this case as a fluorinated polyol. Upon exposure to UV-light, the methacrylic groups allow the photocrosslinking reaction to occur leading to the formation of the solid polymeric film. Fourier-transform infrared (FTIR) spectroscopy was employed to monitor the extent of the photocrosslinking process by evaluating the variation of absorption intensity of the methacrylate C=C stretching signal in the FTIR spectrum (1636 cm^{-1}) at increasing UV-light exposure time (normalized with respect to the carbonyl C=O stretching signal found at 1720 cm^{-1}). As a result, a conversion curve of the photocrosslinking process was constructed by plotting the ratio between the intensity of the 1636 cm^{-1} FTIR signal at a given UV exposure time and prior to irradiation (Fig. 2B). An over 80% conversion is achieved after 60 s of UV-light exposure, indicating a fast crosslinking process potentially suitable for large scale production. It is worth it to note that this conversion may be underestimated due to the difficulty of a correct quantitative evaluation of the low residual C=C stretching band.

Fig. 2 HERE

To include a LS functionality to the UV-cured fluoropolymeric coating, a commercial fluorescent organic dye (Lumogen F Violet 570, BASF – from here on referred to as V570) was employed as luminescent doping species because of its high luminescence quantum yield (> 95%, [37]), high absorption coefficient (0.1125 mg kg^{-1} cm^{-1} at peak absorption in PMMA), and relatively easy processability with polymers [38]. In order to examine the optical properties of the dye-doped UV-cured LS-coating, UV-vis absorption and fluorescence spectra were collected. As shown in Fig. 3A, a broad absorption band is found in the LS-coating in the 325-400 nm range, with an absorption peak centered at 378 nm. The fluorescence spectrum is characterized by a sharp emission centered at 433 nm. These characteristics suggest that the interesting optical features of V570 fluorophore may be exploited to improve the spectral response of DSSC devices in the UV portion of the solar spectrum, where most DSSC dyes perform poorly. In view of this, the indoline-based organic dye D131 (Fig. 3B) was selected as representative Ruthenium-free system to be used in organic DSSC devices in combination with the new V570-doped LS-coating presented in this work. As evident from Fig. 3A, the presence of V570 in the LS-coating allows for improved light harvesting in the 325-400 nm spectral range where D131 shows an absorption minimum, and promotes a 55-nm red-shifted emission in the spectral region where D131 shows an absorption maximum.

Fig. 3 HERE.

To evaluate the effect of this excellent spectral matching on PV performance, DSSC devices were fabricated by sandwiching a D131-sensitized TiO_2 mesoporous anode, an iodide/triiodide liquid electrolyte and a Pt-sputtered counter electrode. The LS film was spin-coated on the external side of PV cell photoanode (Fig. 1A), and the effect of increasing amounts of V570 incorporated in the photopolymer on the performance of the DSSC devices was thoroughly investigated.

The PV response of the LS-DSSC system at increasing V570 concentration is reported in Fig. 4, where the clearly positive effect of the LS-coating on DSSC performance can be noticed on all characteristic PV parameters. To begin with, a strong improvement of short circuit photocurrent density ($J_{sc,}$ Fig. 4A) was achieved. In detail, a 15% J_{sc} enhancement was observed in the presence of 0.75 wt% V570 with respect to uncoated devices, rising up to 135% in the presence of 2 wt% V570 luminophore in the crosslinked polymeric film. These data confirmed that the adopted luminescent material is effectively able to convert at the nanoscale the region of the solar spectrum peaked at 378 nm into lower-energy photons of wavelengths well matching the absorption spectrum of D131 (Fig. 3A). The latter phenomenon is easily noticeable by observing the incident photon-to-current efficiency (IPCE) curves reported in Fig. 5A. Here, the increased amount of photons harvested by the D131 dye due to the presence of the LS-coating led to increased IPCE values in the spectral region where the absorption of the luminophore V570 is centered (378 nm). The optical effect resulting from the incorporation of a LS agent in the new polymeric matrix presented in this work can also be clearly appreciated in Fig. 1B. The integration of the product of the AM1.5G photon flux with the IPCE spectrum yielded predicted J_{sc} values equal to 6.87, 8.04 and 9.25 mA cm^{-2} for the LS-free and LS-coated (0.75 and 2.0 wt%) DSSCs, respectively, which are in excellent agreement with the measured values reported in the photocurrent-photovoltage (J-V) curves in Fig. 5B.

Data reported in Fig. 4A show that a plateau J_{sc} value is reached for V570 concentrations in the 1.5-2 wt% range. With the aim of further investigating the effect of fluorophore concentration and thus extending the experimental domain we also produced DSSC devices incorporating a 5 wt% V570-doped LS coating. However, a decrease of J_{sc} from 9.31 mA cm^{-2} (2 wt% V570) to 8.48 mA cm^{-2} (5 wt% V570) was observed. This behavior may be explained by considering two concurrent effects taking place at increasing fluorophore concentrations. A higher concentration of fluorescent species may increase the probability for an emitted photon to be re-absorbed by another adjacent fluorophore molecule in the LS film, due to the partial overlap between absorption and emission

spectra of V570 dye (Fig. 3A) and because of the decreasing fluorophore-to-fluorophore intermolecular distance with increasing V570 concentration. Additionally, an increased concentration of fluorescent species in the LS coating may result in the formation of molecular aggregates (dimers and excimers), that were shown on similar systems to promote fluorescence quenching [39,40]. These two parallel phenomena may be responsible for a lower amount of fluorescence photons emitted by the LS coating to reach the underlying DSSC photoactive layer for PV conversion, thus leading to a performance (J_{sc}) decrease at higher V570 concentrations. Finally, the progressively higher optical density of the LS coating at increasing V570 concentration may also cause a reduction of the amount of long-wavelength photons reaching the DSSC device due to decreased coating transmittance, ultimately leading to an overall decrease in PV performance. This effect is clearly visible at fluorophore concentrations higher than 2 wt% (see Figure A.1 in the Appendix A).

While the increase of photocurrent density could be reasonably expected in the presence of a LS coating, it was quite surprising to note that also the open-circuit voltage (V_{oc}) was slightly improved with increasing V570 concentration (see Fig. 4B). There is a general agreement within the DSSC scientific community about the dependence of V_{oc} on the electrolyte composition and on the modification of electrodes/electrolyte interfaces [41,42]. However, the same components were used for the fabrication of all the DSSC devices presented in this work, while the only variable was the concentration of the luminescent agent. We speculate that the trend observed on V_{oc} may be due to a thermal effect induced by the presence of the LS coating. Indeed, a decrease of V_{oc} is usually caused by the increase of the dark current attributed to the triiodide reduction by conduction band electrons at the semiconductor-electrolyte junction [43]. Such a process is enhanced when temperature rises. Indeed, in this system the recombination resistance (R_{rec}) follows the relation

$$R_{rec} = R_0 \cdot exp\left(-\frac{\beta \cdot q}{k_B \cdot T} \cdot V_F\right) \quad \text{(Eq. 1)}$$

where β is a coefficient associated with the non-linearity of the charge transfer process and equivalent to the non-ideality factor ($m = \beta^{-1}$) of the diode equation used for standard semiconductor solar cells, q is the electron charge, k_B the Boltzmann constant, T the absolute temperature, V_f the potential drop in the TiO_2 film, and R_0 the pre-exponential parameter which results from the relation

$$R_0 = \frac{T_0 \cdot \sqrt{\pi \cdot \lambda \cdot k_B \cdot T}}{q^2 \cdot L \cdot k_0 \cdot c_{ox} \cdot N_s \cdot T} \cdot exp\left(\frac{E_c - E_{redox}}{k_B \cdot T_0} + \frac{\lambda}{4k_B \cdot T}\right) \quad \text{(Eq. 2)}$$

where λ is the reorganization energy, L the film thickness, k_0 a time constant for tunneling (rate constant), c_{ox} the concentration of acceptor species in the electrolyte, N_s the density of states near the TiO_2 surface, E_c the conduction band position of TiO_2, and T_0 a parameter with temperature units determining the depth of the trap distribution tail under the conduction band [44,45]. This model agrees well with a recombination process occurring through extended surface states in an energy tail distributed below the conduction band, which follows the Marcus probabilistic model [46]. As a consequence, the decrease usually observed in R_{rec} with increasing temperature is associated with a decrease in R_0 and is responsible for the onset of current loss that occurs at lower potentials [47]. Therefore, the increased V_{oc} values observed for the coated DSSCs may be the result of two different phenomena. First, the fluoropolymeric coating deposited on the light-exposed face of the DSSC device is able to absorb hot IR photons of the solar spectrum, thus reducing device operating temperature. Indeed, fluoropolymers are characterized by a strong and wide absorption band in the IR region of the electromagnetic spectrum, which results from the C-F bond stretching vibration [48]. This characteristic behavior may lead to increased R_0 and R_{rec} and in turn to enhanced V_{oc}. As a second effect, the presence of increasing amount of fluorophore in the LS coating partially shields the DSSC device from harmful near UV photons, which are known to cause photo-oxidation of some DSSC components and lead to the formation of radical species or organic by-products that could act as electron acceptors at the electrolyte/photoanode interface [49].

The UV-shielding effect imparted by the LS coating may limit the formation of such electron acceptor species in the electrolyte (c_{ox}), thus resulting in increased R_0, R_{rec} and V_{oc}. Moreover, such a reduction of the recombination phenomena also resulted in a slight improvement of fill factor (*FF*) values (Fig. 4C), as already reported by previous studies about thermal effects on the PV performance [50].

The effect of the LS coating on the PV parameters as described above led to a maximum overall sunlight to electricity conversion efficiency (η) improvement of 62% with respect to uncoated DSSC devices. As reported in Fig. 4D, device performance increased from 2.10% to 3.41% when a 2 wt% V570-laden LS coating was used. To the best of our knowledge, this value represents the highest efficiency enhancement reported so far for organic DSSC systems by means of a polymeric LS layer doped with an organic fluorophore. This very positive result appears even more remarkable when considering that the LS coating has been applied through a cheap, straightforward and easily up-scalable process of light-induced polymerization, carried out at room temperature and without the use of catalysts or separation/purification steps. Moreover, a slight anti-reflective behavior was conferred to the photoanode (see Fig. A.2 in the Appendix A).

For particular purposes, such as flexible PV cells [51], aerospace applications [52] and power stations [53], device transparency is not required. Thus, the use of back-reflective surfaces (BRSs) on the rear of the PV cells may represent an interesting option to increase the photon flux available for the PV device. In fact, if the DSSC components (coating, conductive glass, photoanode, electrolyte and cathode) are sufficiently transparent, the photons unabsorbed by the sensitizer are reflected by the BRS and sent back to the sensitizer. In this work, we also assembled the 2 wt% V570-laden LS-DSSC (η = 3.41%) with a BRS positioned on the counter electrode side. An efficiency as high as 5.02% (J_{sc} = 13.62 mA cm^{-2}, V_{oc} = 0.55 V, *FF* = 0.67) was obtained, thereby confirming the excellent transparency of the LS coating (and also of the other components used for fabricating the DSSC devices) and its suitability to be used in applications in which a BRS is involved [54].

Fig. 4 HERE

Fig. 5 HERE

In addition to providing excellent transparency and relatively good solubility of the fluorescent species, the choice of the new fluoropolymeric coating proposed in this work was also driven by the need of ensuring long-term durability of the operating device. In fact, a decrease in device efficiency is usually observed during the first weeks of DSSC device lifetime, and this issue represents a serious drawback for the widespread application of this technology [55]. In recent years, this aspect has forced the scientific community to propose new materials to reduce the volatility of the liquid electrolyte [56,57] and to protect cell components from the action of UV light, heat and meteorological phenomena [58]. In this context, the use of fluoropolymeric coatings for outdoor applications may represent an interesting approach to ensure high weathering resistance and long-term durability of DSSC devices, due to the excellent weatherability characteristics given to fluorinated polymers by the higher strength of the carbon-fluorine bond compared to the carbon-hydrogen bond [23,33].

With the aim of verifying under real operative conditions the performance of the fluoropolymeric coating presented in this work, an intensive device aging study was carried out. A long-term weathering study on control bare DSSCs and LS-DSSCs was conducted in real outdoor conditions for three months (2140 h), during which the PV cells were exposed (day and night) in the garden of the IIT building in Turin (45°03'42.0"N, 7°39'48.1"E), located in northern Italy in a humid subtropical climate zone. Thanks to this choice, all the DSSC devices were subjected to highly variable climatic conditions, which are particularly useful for our purpose, i.e. to carry out a realistic long-term study of DSSC aging. During the first quarter of 2014 (February-April), outdoor temperatures ranged from -2 to 32 °C and about 350 mm of accumulated rain were measured by the local environmental protection agency (Arpa Piemonte) [59]. The comparison between the aging test on coated (2 wt% V570) and control devices is reported in Fig. 6A. Together with the data

plotted in Fig. 4, it is clear how the proposed luminescent coating not only produced a great improvement of DSSCs performance, but also imparted an excellent long-term stability to the DSSC device under real outdoor conditions, the latter representing an aspect of paramount importance for the practical exploitation of this kind of third generation PV technology. In detail, while the control device (V570 0 wt%) lost about 30% of its initial efficiency, the LS-DSSC system (V570 2.0 wt%) preserved 93% of its starting performance.

The strong improvement of long-term stability under real outdoor conditions observed when the LS coating was applied to the DSSC device may be ascribed to the action of three combined factors. Firstly, the coating showed easy-cleaning properties due to its fluorinated nature. Static contact angle measurements performed on the LS coating to investigate its wettability behavior revealed the fairly hydrophobic character of the new fluoropolymeric coating. As can be appreciated in Fig. 6B, a remarkable increase of water contact angle θ_{H2O} and a decrease of surface tension γ were observed when the outer DSSC glass was coated with the new fluoropolymeric LS system. Such behavior allows to keep the external side of the photoanode clean, thus avoiding the decrease of device photocurrent likely caused by the formation of physical barriers (dust, dirt, water residues) that may prevent incident solar photons from reaching the D131-sensitized electrode for PV conversion. Secondly, the hydrophobic nature of the coating applied on the device may contribute to hinder a very important and widespread degradation phenomenon observed in DSSC systems, i.e. the permeation of water into the device that is often found to alter the composition and the correct functionality of photoanode and electrolyte [60]. Finally, we previously showed that the luminescent species present in the LS coating can act as a light-shifter, thus also serving the function of a UV filter. As a consequence, the remarkable aging resistance shown by the LS-DSSC systems is also attributable to the reduction of the light-induced degradation phenomena normally occurring during outdoor exposure to the photosensitive components of DSSC devices, especially to dye, redox couple and electrolyte additives [61]. The excellent thermal stability of the fluoropolymeric system used as carrier matrix (see Fig. A.3 Appendix A for the thermogravimetric

391 analysis of the coating) combined with its intrinsic photooxidative stability further contribute to
392 enhance the lifetime of LS-DSSC systems.

393 All the present findings clearly highlight the multifunctional nature of the here-proposed LS
394 coating, whose excellent barrier properties to the meteorological phenomena (occurred during the
395 aging test) are also evident from a visual inspection of control and LS-DSSC devices after long-
396 term outdoor exposure (see Fig. A.4 in the Appendix A).

397

398 **Fig. 6** HERE

399

400

401 ## 4. CONCLUSIONS

402 In conclusion, for the first time a fluoropolymeric and rare elements-free LS coating system
403 was designed, synthesized and characterized for use in organic DSSC devices. By the introduction
404 of a fluorescent species in a newly proposed fluoropolymeric matrix, down-shifting of UV photons
405 into valuable visible light has been achieved. As a consequence, DSSCs incorporating the coating
406 system showed an over 60% relative increase in photovoltaic efficiency, mainly caused by the
407 increased photon flux harvested by the organic dye resulting from the nanometric light shifting
408 effect promoted by the luminescent agent. Furthermore, a long-term weathering study was
409 performed under real outdoor conditions, and DSSCs incorporating the LS coating were found to
410 nearly fully preserve their initial power conversion efficiency, as opposed to control devices that
411 showed a 26% relative efficiency loss. Such a remarkable outdoor stability observed for LS-DSSCs
412 was attributed to the multipurpose behavior of the LS layer. Indeed, such new coating system was
413 able to act both as a UV-screening agent (thus preserving the photosensitive PV cell components)
414 and as an easy-cleaning layer (by keeping the PV cell clean and preventing water permeation). This
415 study clearly demonstrates that it is possible to simultaneously improve performance and
416 weatherability of organic DSSC devices, and may be readily extended to a large variety of

sensitizer/luminophore combinations as well as to the nascent world of perovskite solar cells, whose instability to humidity and near-UV radiation represents one of the major problems currently under intense investigation [62].

5. APPENDIX A

Solubility of luminescent species; Anti-reflective properties; Thermal stability of LS coating; DSSC fabrication and visual aspect after aging test.

425 **REFERENCES**
426
427

[1] M. Grätzel, Dye-sensitized solar cells, J. Photochem. Photobiol., C 4 (2003) 145-153.

[2] B. C. O'Regan, M. Grätzel, A low-cost, high-efficiency solar cell based on dye-sensitized colloidal TiO_2 films, Nature 353 (1991) 737-740.

[3] F. Bella, A. Sacco, D. Pugliese, M. Laurenti, S. Bianco, Additives and salts for dye-sensitized solar cells electrolytes: what is the best choice?, J. Power Sources 364 (2014) 333-343.

[4] S. Mathew, A. Yella, P. Gao, R. Humphry-Baker, B. F. E. Curchod, N. Ashari-Astani, I. Tavernelli, U. Rothlisberger, M. K. Nazeeruddin, M. Grätzel, Dye-sensitized solar cells with 13% efficiency achieved through the molecular engineering of porphyrin sensitizers, Nat. Chem. 6 (2014) 242-247.

[5] Y. Duan, Q. Tang, R. Li, B. He, L. Yu, An avenue of sealing liquid electrolyte in flexible dye-sensitized solar cells, J. Power Sources 274 (2015) 304-309.

[6] Z. Wang, Q. Tang, B. He, X. Chen, H. Chen, L. Yu, Titanium dioxide/calcium fluoride nanocrystallite for efficient dye-sensitized solar cell. A strategy of enhancing light harvest, J. Power Sources 275 (2015) 175-180.

[7] W. Guo, X. Xue, S. Wang, C. Lin, Z. L. Wang, An integrated power pack of dye-sensitized solar cell and Li battery based on double-sided TiO_2 nanotube arrays, *Nano Lett.* 12 (2012) 2520-2523.

[8] S. Ahmad, E. Guillén, L. Kavan, M. Grätzel, M. K. Nazeeruddin, Metal free sensitizer and catalyst for dye sensitized solar cells, Energy Environ. Sci. 6 (2013) 3439-3466.

[9] K. Kakiage, Y. Aoyama, T. Yano, T. Otsuka, T. Kyomen, M. Unno, M. Hanaya, An achievement of over 12 percent efficiency in an organic dye-sensitized solar cell, Chem. Commun. 50 (2014) 6379-6381.

[10] K. Ali, S. A. Khan, M. Z. Mat Jafri, Enhancement of silicon solar cell efficiency by using back surface field in comparison of different antireflective coatings, Sol. Energy 101 (2014) 1-7.

[11] P. M. Kaminski, F. Lisco, J. M. Walls, Multilayer broadband antireflective coatings for more efficient thin film CdTe solar cells, IEEE J. Photovoltaics 4 (2014) 452-456.

[12] L. Yao, J. He, Recent progress in antireflection and self-cleaning technology - from surface engineering to functional surfaces, Prog. Mater Sci. 61 (2014) 94-143.

[13] P. Šiffalovič, M. Jergel, M. Benkovičová, A. Vojtko, V. Nádaždy, J. Ivančo, M. Bodík, M. Demydenko, E. Majková, Towards new multifunctional coatings for organic photovoltaics, Sol. Energy Mater. Sol. Cells 125 (2014) 127-132.

[14] L. Miao, L. F. Su, S. Tanemura, C. A. J. Fisher, L. L. Zhao, Q. Liang, G. Xu, Cost-effective nanoporous SiO_2-TiO_2 coatings on glass substrates with antireflective and self-cleaning properties, Appl. Energy 112 (2013) 1198-1205.

[15] N. Jiang, T. Sumitomo, T. Lee, A. Pellaroque, O. Bellon, D. Milliken, H. Desilvestro, High temperature stability of dye solar cells, Sol. Energy Mater. Sol. Cells 119 (2013) 36-50.

[16] J. T. Park, J. H. Kim, D. Lee, Excellent anti-fogging dye-sensitized solar cells based on superhydrophilic nanoparticle coatings, Nanoscale 6 (2014) 7362-7368.

[17] S. Y. Heo, J. K. Koh, G. Kang, S. H. Ahn, W. S. Chi, K. Kim, J. H. Kim, Bifunctional moth-eye nanopatterned dye-sensitized solar cells: light-harvesting and self-cleaning effects, Adv. Energy. Mater. 4 (2014) 1300632.

[18] J. Scheirs, Modern fluoropolymers: high performance polymers for diverse applications, John Wiley & Sons Ltd, Chichester, 1997.

[19] D. M. Lemal, Perspective on fluorocarbon chemistry, J. Org. Chem. 69 (2004) 1-11.

[20] D. O'Hagan, Understanding organofluorine chemistry. An introduction to the C–F bond, Chem. Soc. Rev. 37 (2008) 308-319.

[21] G. Couture, B. Campagne, A. Alaaeddine, B. Ameduri, Synthesis and characterizations of alternating co- and terpolymers based on vinyl ethers and chlorotrifluoroethylene, Polym. Chem. 4 (2013) 1960-1968.

[22] G. Griffini, M. Levi, S. Turri, Novel high-durability luminescent solar concentrators based on fluoropolymer coatings, Progr. Org. Coat. 77 (2014) 528-536.

[23] G. Griffini, M. Levi, S. Turri, Novel crosslinked host matrices based on fluorinated polymers for long-term durability in thin-film luminescent solar concentrators, Sol. Energy Mater. Sol. Cells 118 (2013) 36-42.

[24] G. Griffini, L. Brambilla, M. Levi, C. Castiglioni, M. Del Zoppo, S. Turri, Anthracene/tetracene cocrystals as novel fluorophores in thin-film luminescent solar concentrators, RSC Adv. 4 (2014) 9893-9897.

[25] F. Bella, R. Bongiovanni, R. S. Kumar, M. A. Kulandainathan, A. M. Stephan, Light cured networks containing metal organic frameworks as efficient and durable polymer electrolytes for dye-sensitized solar cells, J. Mater. Chem. A 1 (2013) 9033-9036.

[26] J. D. Douglas, G. Griffini, T. W. Holcombe, E. P. Young, O. P. Lee, M. S. Chen, J. M. J. Fréchet, Functionalized isothianaphthene monomers that promote quinoidal character in donor-acceptor copolymers for organic photovoltaics, Macromolecules 45 (2012) 4069-4074.

[27] G. Griffini, J. D. Douglas, C. Piliego, T. W. Holcombe, S. Turri, J. M. J. Fréchet, J. L. Mynar, Long-term thermal stability of high-efficiency polymer solar cells based on photocrosslinkable donor-acceptor conjugated polymers, Adv. Mater. 23 (2011) 1660-1664.

[28] M. N. Huang, Y. Y. Ma, F. Xiao, Q. Y. Zhang, Bi^{3+} sensitized $Y_2WO_6:Ln^{3+}$ (Ln = Dy, Eu, and Sm) phosphors for solar spectral conversion, Spectrochim. Acta, Part A 120 (2014) 55-59.

[29] Z. Hosseini, W. K. Huang, C. M. Tsai, T. M. Chen, N. Taghavinia, E. W. Diau, Enhanced light harvesting with a reflective luminescent down-shifting layer for dye-sensitized solar cells, ACS Appl. Mater. Interfaces 5 (2013) 5397-5402.

[30] Y. Li, K. Pan, G. Wang, B. Jiang, C. Tian, W. Zhou, Y. Qu, S. Liu, L. Feng, H. Fu, Enhanced photoelectric conversion efficiency of dye-sensitized solar cells by the incorporation of dual-mode luminescent $NaYF_4:Yb^{3+}/Er^{3+}$, Dalton Trans. 42 (2013) 7971-7979.

[31] J. Wang, J. Wu, J. Lin, M. Huang, Y. Huang, Z. Lan, Y. Xiao, G. Yue, S. Yin, T. Sato, Application of $Y_2O_3:Er^{3+}$ nanorods in dye-sensitized solar cells, ChemSusChem 5 (2012) 1307-1312.

[32] J. Liu, Q. Yao, Y. Li, Effects of downconversion luminescent film in dye-sensitized solar cells, Appl. Phys. Lett. 88 (2006) 173119.

[33] G. Griffini, F. Bella, F. Nisic, C. Dragonetti, D. Roberto, M. Levi, R. Bongiovanni, S. Turri, Multifunctional luminescent down-shifting fluoropolymer coatings: a straightforward strategy to improve the UV-light harvesting ability and long-term outdoor stability of organic dye-sensitized solar cells, Adv. Energy Mater., DOI: 10.1002/aenm.201401312.

[34] L. Y. Lin, M. H. Yeh, C. P. Lee, J. Chang, A. Baheti, R. Vittal, K. R. Justin Thomas, K. C. Ho, Insights into the co-sensitizer adsorption kinetics for complementary organic dye-sensitized solar cells, J. Power Sources 247 (2014) 906-914.

[35] S. Kumar Swami, N. Chaturvedi, A. Kumar, R. Kapoor, V. Dutta, J. Frey, T. Moehl, M. Grätzel, S. Mathew, M. K. Nazeeruddin, Investigation of electrodeposited cobalt sulphide counter electrodes and their application in next-generation dye sensitized solar cells featuring organic dyes and cobalt-based redox electrolytes, J. Power Sources 275 (2015) 80-89

[36] S. K. Pathak, A. Abate, T. Leijtens, D. J. Hollman, J. Teuscher, L. Pazos, P. Docampo, U. Steiner, H. J. Snaith, Towards long-term photostability of solid-state dye sensitized solar cells, Adv. Energy. Mater. 4 (2014) 1301667.

[37] D. Ross, E. Klampaftis, J. Fritsche, M. Bauer, B. S. Richards, Increased short-circuit current density of production line CdTe mini-module through luminescent down-shifting, Sol. Energy Mater. Sol. Cells 103 (2012) 11-16.

[38] L. R. Wilson, B. S. Richards, Measurement method for photoluminescent quantum yields of fluorescent organic dyes in polymethyl methacrylate for luminescent solar concentrators, Appl. Opt. 48 (2009) 212-220.

[39] R. O. Al Kaysi, T. S. Ahn, A. M. Muller, C. J. Bardeen, The photophysical properties of chromophores at high (100 mM and above) concentrations in polymers and as neat solids, Phys. Chem. Chem. Phys. 8 (2006) 3453-3459.

[40] H. Yoo, J. Yang, A. Yousef, M. R. Wasielewski, D. Kim, Excimer formation dynamics of intramolecular pi-stacked perylenediimides probed by single-molecule fluorescence spectroscopy, J. Am. Chem. Soc. 132 (2010) 3939-3944.

[41] T. Chen, L. Qiu, Z. Cai, F. Gong, Z. Yang, Z. Wang, H. Peng, Intertwined aligned carbon nanotube fiber based dye-sensitized solar cells, Nano Lett. 12 (2012) 2568-2572.

[42] S. J. Park, K. Yoo, J. Y. Kim, J. Y. Kim, D. K. Lee, B. S. Kim, H. Kim, J. H. Kim, J. Cho, M. J. Ko, Water-based thixotropic polymer gel electrolyte for dye-sensitized solar cells, ACS Nano 7 (2013) 4050-4056.

[43] G. Boschloo, A. Hagfeldt, Characteristics of the iodide/triiodide redox mediator in dye-sensitized solar cells, Acc. Chem. Res. 42 (2009) 1819-1826.

[44] Q. Wang, S. Ito, M. Grätzel, F. Fabregat-Santiago, I. Mora-Serò, J. Bisquert, T. Bessho, H. Imai, Characteristics of high efficiency dye-sensitized solar cells, J. Phys. Chem. B 110 (2006) 19406-19411.

[45] S. R. Raga, F. Fabregat-Santiago, Temperature effects in dye-sensitized solar cells, Phys. Chem. Chem. Phys. 15 (2013) 2328-2336.

[46] R. Memming, Semiconductor Electrochemistry, Wiley-VCH, Weinheim, 2001.

[47] F. Fabregat-Santiago, G. Garcia-Belmonte, I. Mora-Serò, J. Bisquert, Characterization of nanostructured hybrid and organic solar cells by impedance spectroscopy, Phys. Chem. Chem. Phys. 13 (2011) 9083-9118.

[48] G. Hougham, P. E. Cassidy, K. Johns, T. Davidson, Fluoropolymers 2. Properties, Kluwer Academic/Plenum Publishers, Dordrecht, 1999.

[49] S. Mastroianni, I. Asghar, K. Miettunen, J. Halme, A. Lanuti, T. M. Brown, P. Lund, Effect of electrolyte bleaching on the stability and performance of dye solar cells, Phys. Chem. Chem. Phys. 16 (2014) 6092-6100.

[50] P. J. Li, J. H. Wu, M. L. Huang, S. C. Hao, Z. Lan, Q. Li, S. Kang, The application of P(MMA-co-MAA)/PEG polyblend gel electrolyte in quasi-solid state dye-sensitized solar cell at higher temperature, Electrochim. Acta 53 (2007) 903-908.

[51] F. Bella, A. Lamberti, A. Sacco, S. Bianco, A. Chiodoni, R. Bongiovanni, Novel electrode and electrolyte membranes: towards flexible dye-sensitized solar cell combining vertically aligned TiO_2 nanotube array and light-cured polymer network, J. Membr. Sci. 470 (20149 125-131.

[52] J. D. Harris, E. J. Anglin, A. F. Hepp, S. G. Bailey, D. A. Scheiman, S. L. Castro, Space environmental testing of dye-sensitized solar cells, Eur. Space Agency Spec. Publ. SP 502 (2002) 629-632.

[53] S. Dai, J. Weng, Y. Sui, S. Chen, S. Xiao, Y. Huang, F. Kong, X. Pan, L. Hu, C. Zhang, K. Wang, The design and outdoor application of dye-sensitized solar cells, Inorg. Chim. Acta 2008, 361, 786-791.

[54] V. Zardetto, F. Di Giacomo, D. Garcia-Alonso, W. Keuning, M. Creatore, C. Mazzuca, A. Reale, A. Di Carlo, T. M. Brown, Fully plastic dye solar cell devices by low-temperature UV-irradiation of both the mesoporous TiO_2 photo- and platinized counter-electrodes, Adv. Energy Mater. 3 (2013) 1292-1298.

[55] L. Tao, Z. Huo, S. Dai, J. Zhu, C. Zhang, Y. Huang, B. Zhang, J. Yao, Stable quasi-solid-state dye-sensitized solar cell using a diamide derivative as low molecular mass organogelator, J. Power Sources 262 (2014) 444-450.

[56] X. Wang, S. A. Kulkarni, B. I. Ito, S. K. Batabyal, K. Nonomura, C. C. Wong, M. Grätzel, S. G. Mhaisalkar, S. Uchida, Nanoclay gelation approach toward improved dye-sensitized solar cell efficiencies: an investigation of charge transport and shift in the TiO_2 conduction band, *ACS Appl. Mater. Interfaces* 5 (2013) 444-450.

[57] A. Hess, G. Barber, C. Chen, T. E. Mallouk, H. R. Allcock, Organophosphates as solvents for electrolytes in electrochemical devices, *ACS Appl. Mater. Interfaces* 5 (2013) 13029-13034.

[58] K. Darowicki, M. Szociński, K. Schaefer, D. J. Mills, The influence of UV light on performance of poly(methyl methacrylate) in regard to dye-sensitised solar cells, ECS Trans. 24 (2010) 127-136.

[59] Arpa Piemonte [Regional agency for environmental protection] website, http://www.arpa.piemonte.it/rischinaturali/tematismi/clima/rapporti-di-analisi/Eventi.html, accessed: June, 2014.

[60] Y. Liu, A. Hagfeldt, X. R. Xiao, S. E. Lindquist, Investigation of influence of redox species on the interfacial energetics of a dye-sensitized nanoporous TiO_2 solar cell, Sol. Energy Mater. Sol. Cells 55 (1998) 267-281.

[61] J. S. Lissau, D. Nauroozi, M. P. Santoni, S. Ott, J. M. Gardner, A. Morandeira, Anchoring energy acceptors to nanostructured ZrO_2 enhances photon upconversion by sensitized triplet-triplet annihilation under simulated solar flux, J. Phys. Chem. C 117 (2013) 14493-14501.

[62] M. A. Green, A. Ho-Baillie, H. J. Snaith, The emergence of perovskite solar cells, Nat. Photonics 8 (2014) 506-514.

Fig. 1 A) Graphical representation of the working principle of the LS system presented in this work when applied on a DSSC device; **B)** Comparison between a coating-free and a V570-doped LS-DSSC when irradiated with UV light.

Fig. 2 A) Schematic representation of the reaction between the fluorinated polyol (CTFE-VE) and the functional isocyanate (IEM) used for the preparation of the UV-curable fluorinated precursor; **B)** Conversion curve for the photocuring process of the LS-coating. The inset shows the FTIR spectra of the photocurable precursor at increasing UV-exposure times in the 1800-1600 cm^{-1} region, indicating the FTIR peaks associated with C=C (1636 cm^{-1}) and C=O (1720 cm^{-1}) stretching vibrations.

Fig. 3 A) Normalized absorption and emission spectra of the LS-coating presented in this work. The absorption of the organic dye D131 and the AM 1.5G solar emission spectrum are also shown; **B)** Chemical structure of the organic sensitizer D131 used in this work for the fabrication of DSSC devices.

Fig. 4 Variation of PV parameters of LS-DSSC devices at increasing concentration of V570 luminescent species: **A)** Short circuit current density (J_{sc}); **B)** Open circuit voltage (V_{oc}); **C)** Fill factor (FF); **D)** Efficiency (η).

Fig. 5 A) IPCE curves of LS-DSSCs at increasing concentration of V570 luminescent species; **B)** J-V curves of LS-DSSCs at increasing concentration of V570 luminescent species. Reported J_{sc} and V_{oc} values are expressed in mA cm^{-2} and V, respectively.

Fig. 6 A) Stability test carried out on LS-free and LS-coated (2 wt% V570) DSSCs in real outdoor conditions. The lower part of the graph shows the outdoor temperatures (minimum and maximum) registered during the testing period, while the violet curve shows the accumulated rainfall; **B)** Static contact angles (θ_{H2O}) and total surface tension values (γ) for bare glass and glass coated with the LS film.

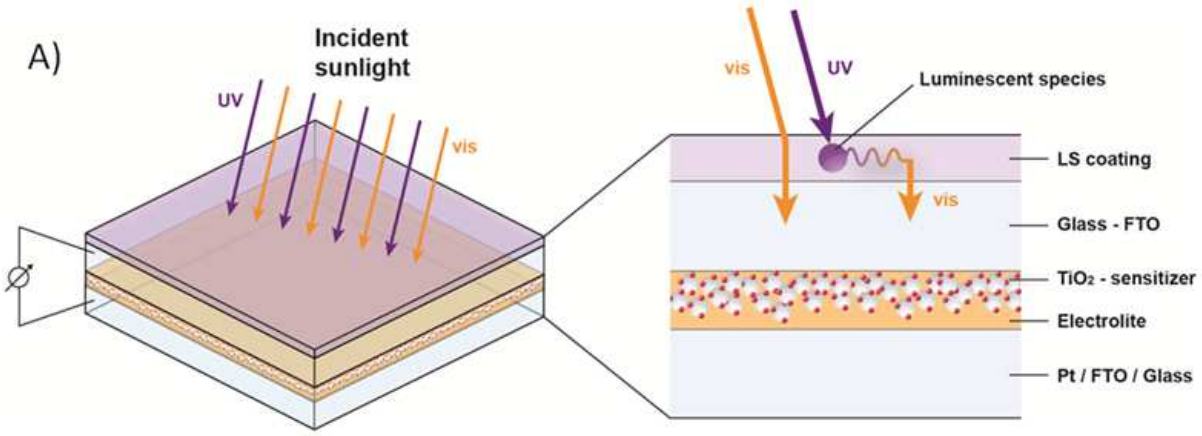

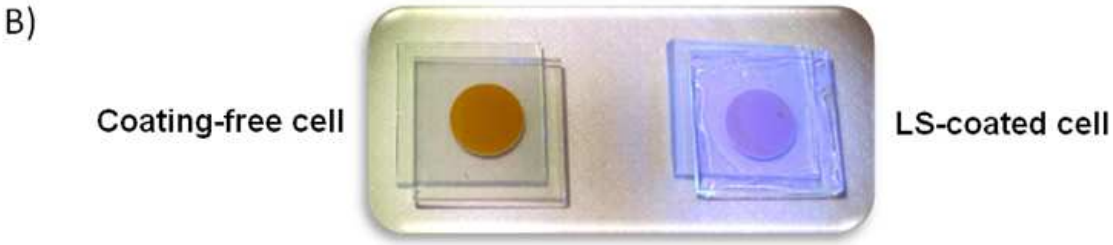

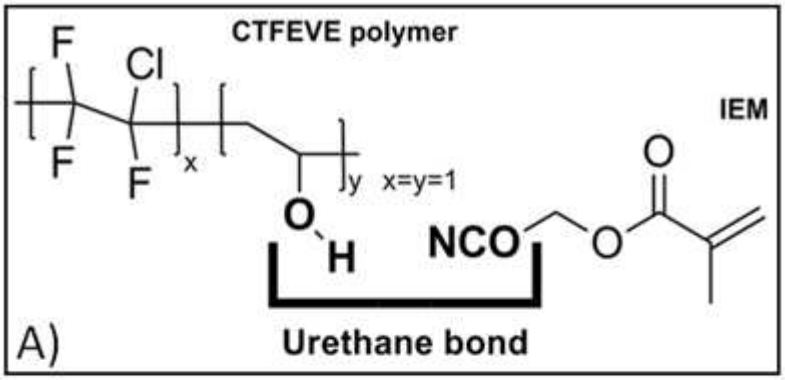

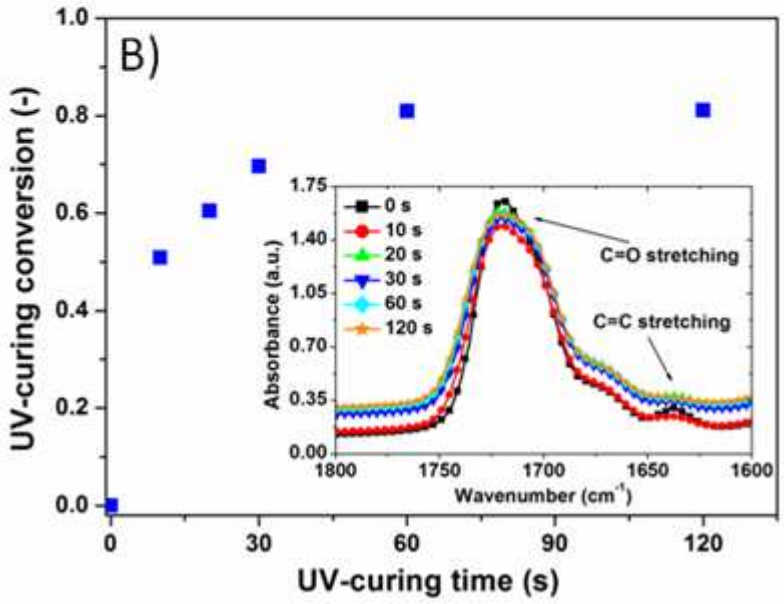

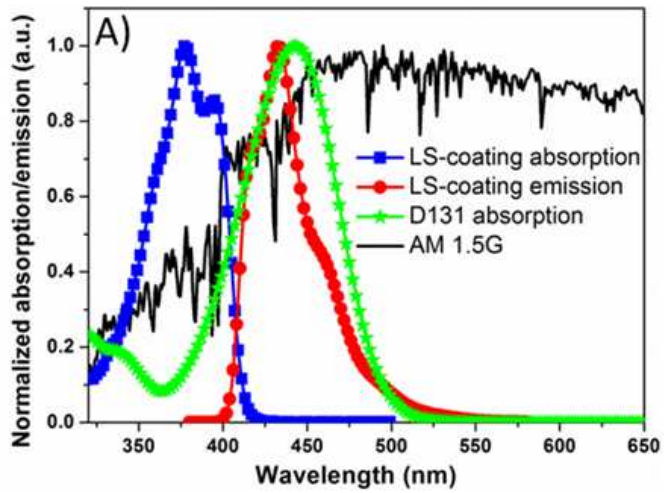

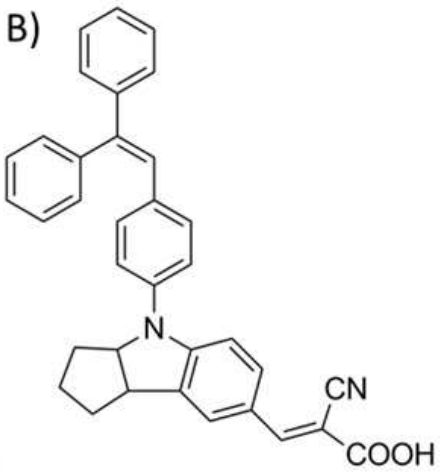

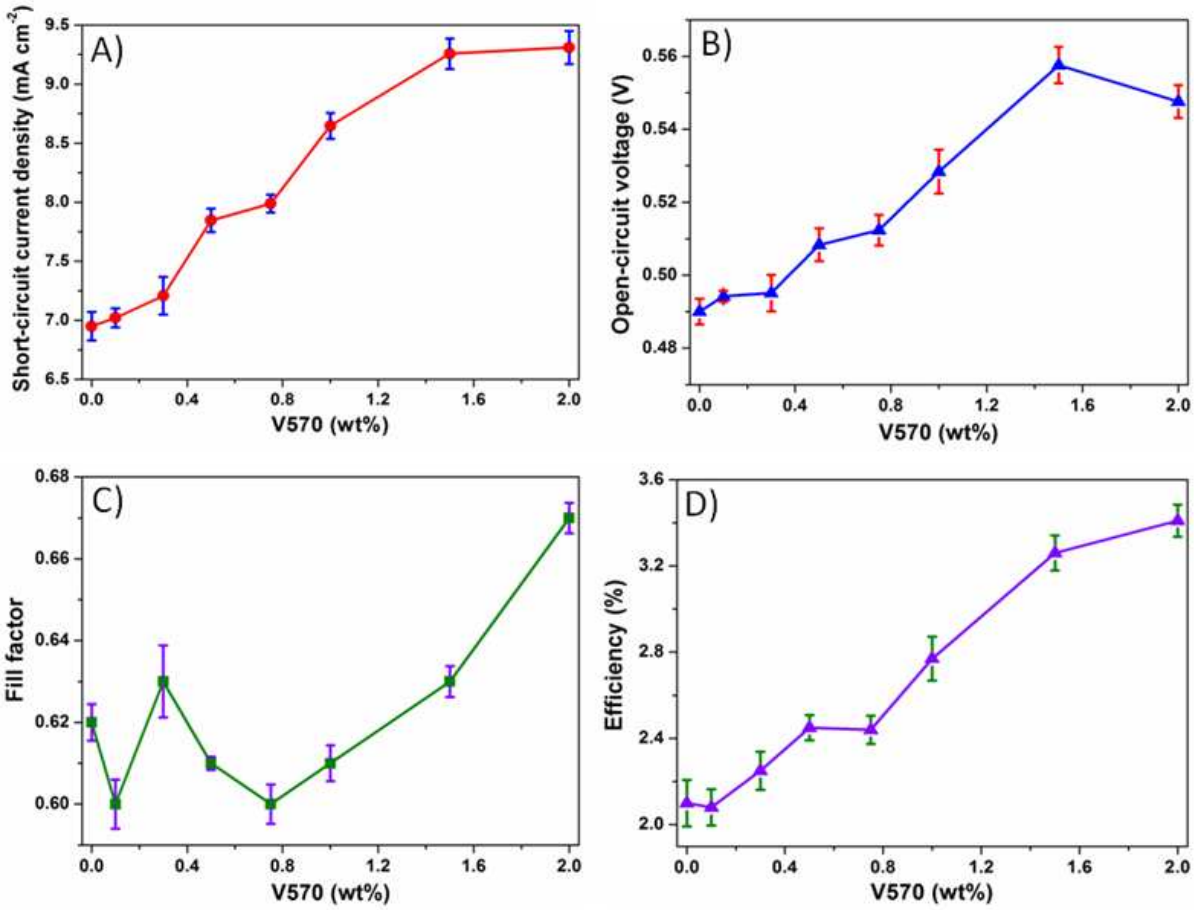

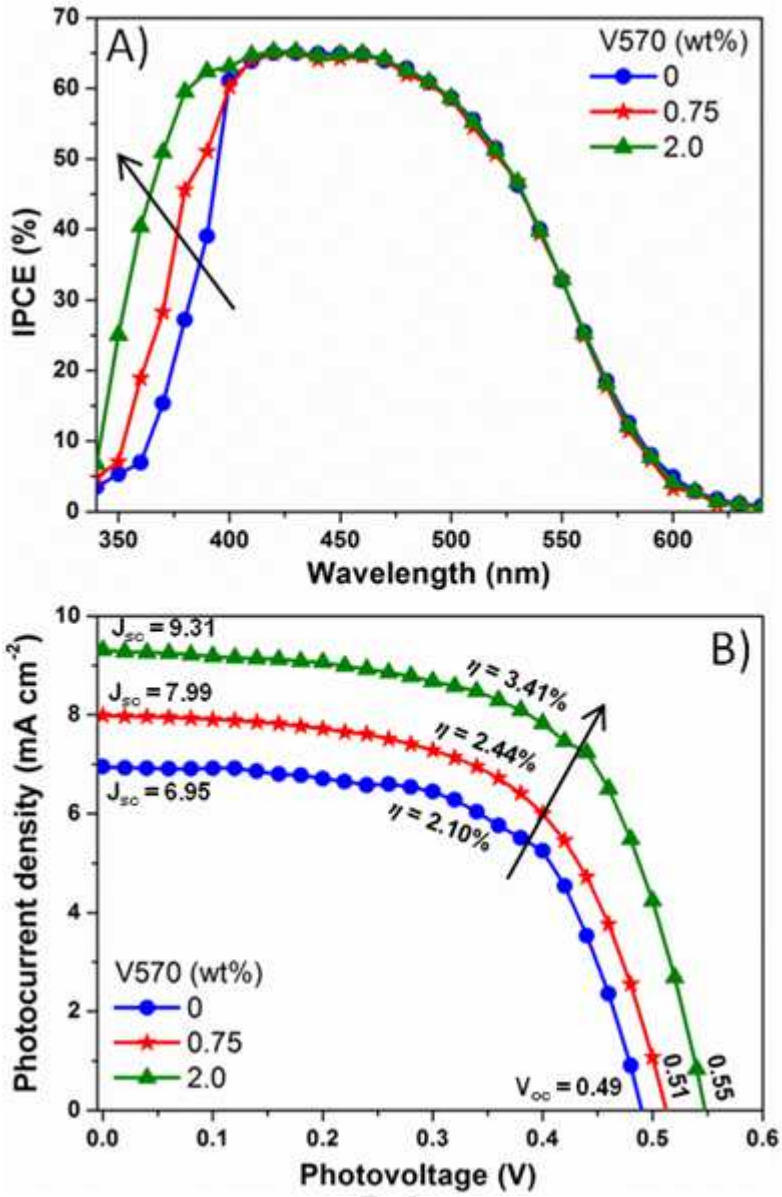

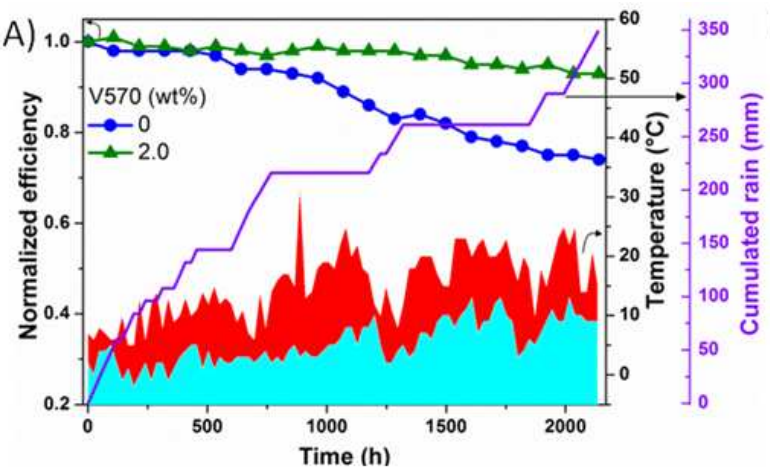

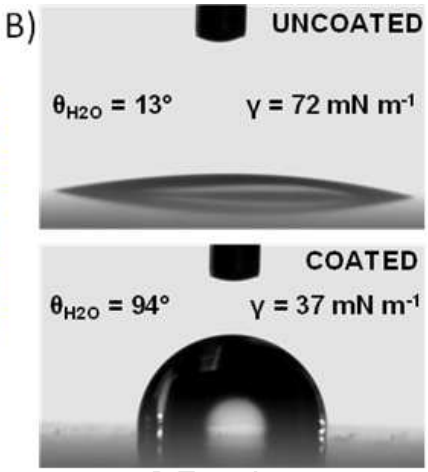

- A multifunctional photocurable fluoropolymeric light-shifting coating is proposed
- A luminescent agent in the coating shifts near-UV photons to VIS wavelengths
- A 60% improvement of the DSSC efficiency was measured
- An aging test was carried out outdoor for more than 2000 hours
- Light-shifting coating allows both efficiency and stability improvements

Performance and stability improvements for dye-sensitized solar cells in the presence of luminescent coatings

Federico **Bella**,[*,1] Gianmarco **Griffini**,[2] Matteo **Gerosa**,[1] Stefano **Turri**,[2] and Roberta **Bongiovanni**[1]

1) Department of Applied Science and Technology - DISAT, Politecnico di Torino, Corso Duca degli Abruzzi 24, 10129 Torino, Italy

2) Department of Chemistry, Materials and Chemical Engineering "Giulio Natta", Politecnico di Milano, Piazza Leonardo da Vinci 32, 20133 Milano, Italy

[*] Corresponding author: Federico Bella (E-mail federico.bella@polito.it; Tel: +39 0110904638; Contact details: affiliation 1)

SUPPORTING INFORMATION

A.1 Solubility of luminescence species

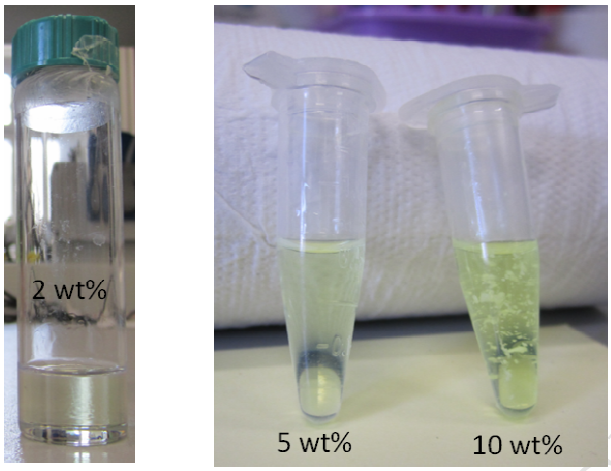

Fig. A.1 Photographs showing the decreased transmittance of the photopolymer precursor mixture when the concentration of the luminescent species (V570) is increased from 2 wt% (left) to 5 wt% (center) and 10 wt% (right).

A.2 Anti-reflective properties

In order to evaluate the anti-reflective properties of the luminescent systems proposed in this work, diffuse reflectance measurements were performed on the coating and the results are presented in Fig. A.2. As shown in the spectrum, the addition of the fluoropolymeric coating reduced the diffuse reflectance of the system by approximately 4% as compared with bare uncoated glass. This indicated that the proposed system could also partially act as antireflective coating, as expected from the lower refractive index of the fluoropolymer employed in this work compared with glass (n=1.438 and n=1.523 for the fluoropolymer and for glass, respectively). However, it is worth to note that such improvement in the antireflective properties cannot be fully responsible for the improvement in the photovoltaic performance of the DSSC device. Indeed, as clearly demonstrated by IPCE measurements of coated DSSC devices (see Figure 5A in the Manuscript), an increased amount of UV photons is made available to the D131 dye due to the down-shifting effect resulting from the presence of the LS-coating, leading to increased IPCE values in the spectral region where the absorption of the luminophore V570 is centered (378 nm).

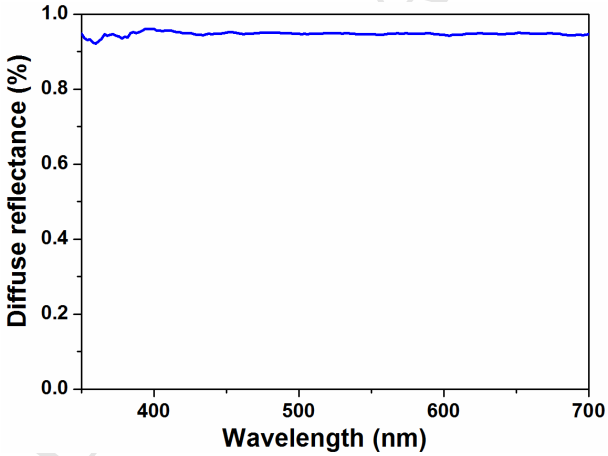

Fig. A.2 Diffuse reflectance spectrum of the coated glass (uncoated glass is used as a reference).

A.3 Thermal stability

The thermo-oxidative stability of the UV-cured LS coating was investigated by means of thermo-gravimetric analysis (TGA) in air (Fig. A.3). A three-stage thermal degradation behavior was observed, with a first weight loss of about 10% occurring in the 100-200 °C temperature range, which was ascribed to cleavage of the urethane bonds.[1] A second major weight loss (70%) was found in the 250-450 °C region, and was attributed to the decomposition of ether and ester linkages and to chain scission reactions,[2,3] which are known to occur in acrylate polymers *via* a free-radical mechanism upon heating in air. Finally, the third weight-loss peak was observed above 470 °C, and indicated the complete decrosslinking and thermal degradation of the polymer.

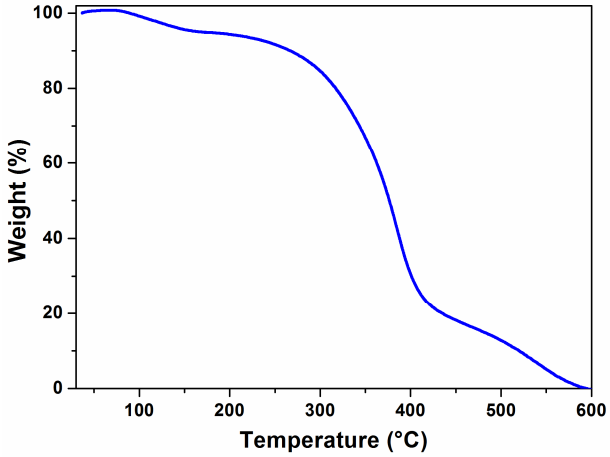

Fig. A.3 TGA thermogram of the LS coating containing 1 wt% V570.

A.4 Visual aspect of DSSC devices after aging test

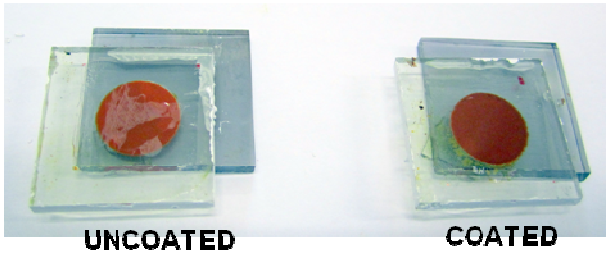

Fig. A.4 Photograph of control (uncoated) and LS-coated DSSC devices after 2140 h of exposure to real outdoor conditions. The control device shows the presence of dirty areas and water residues on the top surface, which are not detected on the LS-coated device.

(1) Kayaman-Apohan, N.; Demirci, R.; Cakir, M.; Gungor, A. UV-Curable Interpenetrating Polymer Networks Based on Acrylate/Vinylether Functionalized Urethane Oligomers. *Radiat. Phys. Chem.* **2005**, *73*, 254-262.

(2) Lin, W. C.; Yang, C. H.; Wang, T. L.; Shieh, Y. T.; Chen, W. J. Hybrid Thin Films Derived From UV-Curable Acrylate-Modified Waterborne Polyurethane and Monodispersed Colloidal Silica. *eXPRESS Polym. Lett.* **2012**, *6*, 2-13.

(3) Mita, I. In *Aspects of Degradation and Stabilization of Polymers*; Jellinek, H. H. G., Ed.; Elsevier: Amsterdam, 1978; Chapter 2, p 47.